An innovative strategy for a step-by-step SFS reconstruction based on variational approach

MonicaCarfagni, Luca Puggelli

***Abstract*—**The stylistic design of new industrial products often starts from shaded handmade sketches which, usually, need to be converted into 3D digital models by using CAD software packages for the subsequent design phases. This conversion often represents the bottleneck of the whole development process. Shape from Shading (SFS), which attempts to recover the 3D geometry of an object starting from a single shaded representation, is potentially capable of speeding-up the 3D conversion. However, existing approaches prove to be extremely unstable and error prone mainly due to the under-determination of the SFS problem. In order to increase the performance of shading based reconstruction authors propose a step-by-step variational-based approach. In particular, the problem is solved into multiple steps, each one providing the initialization for the following, so that the solution gradually converges towards the final surface. Tested against a set of case studies, the method proved its effectiveness.

***Keywords*—**Shape from shading, variational approach, 3D design, stylistic content, Computer Aided Design, Numerical Optimization.

I. Introduction

COMPUTERAided Design software packages are universally recognized as essential to simplify and speed up all the development phases of new industrial products, from design to manufacturing. For this reason, projects usually start at the computer. However, this may not always occur: products characterized by a strong stylistic content, such as jewels, fashion accessories, ceramics, house-ware, plaques and coins are often designed by producing a set of handmade drawings or sketches. In order to take advantage of benefits related to the use of the computer, handmade sketches are manually drafted using a CAD package so as to obtain 3D virtual models better resembling the expected aspect of the final product. This process, usually needing close interaction between stylist and CAD operators, is inevitably time consuming. In order to confront with this issue, in the last few years a number of computer-based methods have been devised with the aim of speeding up the 3D reconstruction process from single images or sketches [1-4]. In case the three-dimensionality of the shape is given by shading, the most important class of methods for retrieving the 3D model is the so called Shape-from-Shading (SFS). SFS allows to recover a proper surface that generates, under the same lighting condition, the same image as the original one, given in input.
Extensively reviewed in [5, 6], SFS methods are based on the analysis of the relation between the brightness of a pixel in the digital image and the incidence angle of light beams with the represented surface. The equation that expresses such relationship, called irradiance equation, is formulated by using three alternative types of unknown:

1. the depth map $Z(i,j)$ which represents the surface height for each pixel (i,j);
2. the surface normal $\vec{N} = [n_x, n_y, n_z]$ which represents the surface normal for the generic pixel (i,j);
3. the surface gradient $\nabla Z = \left[\frac{\partial Z}{\partial x}, \frac{\partial Z}{\partial y}\right] = (p,q)$, that represents the rate of change of depth in x and y directions.

In order to simplify the reconstruction problem, the following hypotheses are usually made:
1) the reflectance model is Lambertian, i.e. the surface is supposed to be homogeneous and completely diffusing. As a consequence, the brightness of each pixel depends only on the light direction and on the surface orientation;
2) perspective is absent and the focal length of the "observer" is set at infinity;
3) the light source is set at infinity i.e. light beams are uniform and parallel each other. This gives the assumption that the light source can be expressed by a single vector for all the pixels.
Under these assumptions, it is possible to relate brightness and surface orientation, in terms of surface normals as follows:

$$I(i,j) = \vec{N}(i,j) \cdot \vec{L} = n_x l_x + n_y l_y + n_z l_z \qquad (1)$$

where:

- $I(i,j)$ is the image (size $n \times m$) representing the shaded object whose surface is to be retrieved (i.e. the input image);
- (i,j) are the coordinates of the generic pixel;

M. Carfagni is with the Department of Industrial Engineering University of Florence (Italy), via di Santa Marta, 3 50139, Firenze (Italy). Phone: (+39) 0552758731; fax: (+39)0552758755; e-mail: monica.carfagni@unifi.it.
L. Puggelli is with the Department of Industrial Engineering University of Florence (Italy), via di Santa Marta, 3 50139, Firenze (Italy).

- $\vec{\mathrm{L}} = [\mathrm{l_x}, \mathrm{l_y}, \mathrm{l_z}]$ is the unit-vector opposed to light direction;

All the normals that solve Eq. 1 lay on the lateral surface of a tipped cone (see Figure 1), whose axis coincides with the vector $\vec{L}$ and whose aperture is proportional to the pixel brightness:

$$\beta = \cos^{-1}(I(i,j)) \tag{2}$$

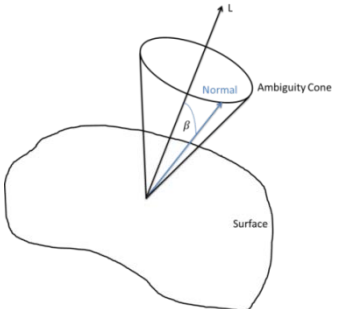

Figure 1 - Cone of ambiguity

Eq. 1, where the unknown is the vector $\vec{N}$, is usually expressed in terms of gradient ∇z [7-9]. The resulting equation is a first order non-linear partial differential equation (PDE) of the Hamilton-Jacobi type, called *fundamental equation of shape from shading* (Eq. 3):

$$I(i,j)\sqrt{1+|\nabla z|^2} + \left(l_\mathrm{x}, l_\mathrm{y}\right)\cdot \nabla z - l_\mathrm{z} = 0 \tag{3}$$

If the light source is frontal, i.e. $\vec{\mathrm{L}} = [0\ 0\ 1]$, the problem is simplified and the equation is then reduced to the well-known "eikonal" form expressed by:

$$I(i,j)\sqrt{1+|\nabla z|^2} - l_\mathrm{z} = 0 \tag{4}$$

Whichever is the selected unknown ($\vec{N}$ or ∇z) the SFS problem results underdetermined. In fact, to each surface point correspond two (p, q) or three $([\mathrm{n_x}, \mathrm{n_y}, \mathrm{n_z}])$ unknowns, while the image provides only one grey value (and so only one equation). For this reason the problem does not have a unique solution, thus all the SFS methods proposed in literature are based on strong assumptions aiming to reduce the complexity in retrieving a suitable 3D surface.

According to scientific literature, it is possible to collect them in four groups: direct approaches [10, 11], local approximation [12], linear approximation [13, 14] and minimization-based approaches [15 - 17].

This last class, used in the present work, is mainly based on hypothesis that the expected surface coincides with the minimum of an appropriate functional F, which consists of the linear combination of few contributions, called constraints.

The main constraints, widely used in literature, are the following: brightness constraint (BC), integrability constraint (IC) and smoothness constraint (SC). Accordingly, in general, the functional F to be minimized is provided by the following equation:

$$F = BC + \lambda SC + \mu IC \tag{5}$$

Where λ and μ are respectively the weights for the Smoothness Constraint and the Integrability Constraint.Minimization approach is known to be the most robust one in case of noisy images [6]. Recent developments [18, 19] showed that, under few easy-to-set boundary conditions, this strategy provides satisfactory results, especially when the input image is a sketch.In any case, the effectiveness of local-minimization algorithms is strongly affected by the initialization given to the iterative minimization process. A proper initialization is crucial for retrieving surfaces reliably resembling the expected one since it allows a better convergence to the global minimum. The method proposed in this paper introduces an original minimization-based variational approach where the reconstruction problem is split into a sequence of SFS sub-problems, each one providing the initialization for the following step.

In particular, from the input image a set of *k* new images are derived by progressively increasing brightness. Then, a first-attempt surface is reconstructed starting from the brightest image by using a planar initialization. Such a surface is used as initialization for the subsequent image (i.e. the second brightest image). The procedure is iterated until the input image is processed i.e. each intermediate step provides the initialization for the following one.

In view of its application to handmade drawings, this work preliminary analyses the applicability of SFS to synthetic images seeking to improve, among the existing ones, the techniques based on minimization approach which are known to more robust in case of inexact shading (like the ones in handmade drawings).

II. Method

As already stated, variational approaches are aimed to minimize the Functional of Eq. 5, mainly based on the definition of three constraints. The most important one is the so called Brightness Constraint (BC). Derived directly from the *irradiance equation* (Eq. 1) this term points out the error between the reconstructed image and the original one:

$$\begin{aligned} BC &= \iint (I(i,j) - \tilde{I}(i,j))^2 dxdy \\ &\cong \sum_{(i,j)\in\Omega} \left(I(i,j) - \tilde{I}(i,j)\right)^2 \end{aligned} \tag{6}$$

where Ω is the image domain.
Since, as already mentioned, Eq. 1 is underdetermined, the minimization of BC cannot help in detecting a unique solution. For this reason, it is necessary to introduce other two constraints. The first one is the Smoothness Constrain (SC); it imposes that the slope of the reconstructed surface changes gradually from a given pixel to its neighbourhood, so that the result appears as smooth as possible, penalizing large local changes in the surface orientation.SC is defined as follows (Eq. 7 and Eq. 8):

$$\begin{aligned} SC &= \iint \left(\left\| \vec{N}_x \right\|^2 + \left\| \vec{N}_y \right\|^2 \right) dxdy \\ &\cong \sum_{(i,j)\in\Omega} \left\| \vec{N}(i+1,j) - \vec{N}(i,j) \right\|^2 \\ &+ \left\| \vec{N}(i,j+1) - \vec{N}(i,j) \right\|^2 \end{aligned} \tag{7}$$

Consequently:

$$\begin{aligned} SC = \sum_{(i,j)\in\Omega} & \left(n_x(i+1,j) - n_x(i,j) \right)^2 + \left(n_y(i+1,j) - n_y(i,j) \right)^2 \\ &+ \left(n_z(i+1,j) - n_z(i,j) \right)^2 \\ &+ \left(n_x(i,j+1) - n_x(i,j) \right)^2 \\ &+ \left(n_y(i,j+1) - n_y(i,j) \right)^2 \\ &+ \left(n_z(i,j+1) - n_z(i,j) \right)^2 \end{aligned} \tag{8}$$

The second constraint is the Integrability Constraint (IC); it provides surfaces that can be integrated, i.e. for any point of the surface, the height is independent from the path of integration [20, 21]. The univocal relation between normal map and height results as follows:

$$\begin{aligned} IC = \iint \left(\frac{\partial p}{\partial y} - \frac{\partial q}{\partial x} \right)^2 dxdy \\ \cong \sum_{(i,j)\in\Omega} & \left[\left(p(i,j+1) - p(i,j) \right) \right. \\ &+ \left(p(i+1,j+1) - p(i+1,j) \right) \\ &- \left(q(i+1,j) - q(i,j) \right) \\ &\left. - \left(q(i+1,j+1) - q(i,j+1) \right) \right]^2 \end{aligned} \tag{9}$$

Once the constraints are defined, the variational approach aims to solve the following equation:

$$min(BC + \lambda \cdot SC + \mu \cdot IC \tag{10}$$

The minimization process makes use of a wide range of algorithms, such as for instance Gauss-Seidel, gradient-based ones or heuristic techniques [5]; however, a number of boundary conditions have to be satisfied to guide the convergence to a feasible solution.
In this work, boundary conditions are selected according to [18] (where an interactive procedure is developed) as briefly recalled below:

1. Morphology-based boundary condition: it requires to select which white regions in the input image correspond to local maxima or minima of the surface, seen parallel to the light direction. The normals on the outline of these areas are displaced radially, pointing outward in case of a maximum or inward in case of a minimum.
2. Background boundary condition: it imposes that the background of the scene, once rebuilt, results perfectly horizontal. It is done by fixing the normals as vertical for each background pixel.
3. Silhouette boundary condition: if the surface is clearly disconnected from the background, user can set the value of the normal around its contour as outward vector.
4. White points boundary condition: the only possible orientation for a pixel to have maximum brightness (i.e. white tone) is that the relative normal $\vec{N}$ is aligned with $\vec{L}$. Therefore, the only possible solution for white pixels is that $\vec{N}$ is coincident with $\vec{L}$ (see [22, 23]).

As long as the typical optimization methods for SFS are local, the initialization is a nodal point: the success of the optimization method derives largely from the initial point of the procedure that is the surface from which the optimization algorithm starts. A typical starting point is the plane perpendicular to the light direction. It is important to note that this plane satisfies automatically all the white areas of the image.The proposed method aims to solve the problem using a step-by-step approach. Each step provides the initialization for the following one, so that the problem of finding a "proper" initialization for the general problem is overcame. Actually, all of the steps – with exception of the final one – have the main aim of recovering the initialization for the original problem.
The general problem is, hence, broken down into SFS sub-problems, each one "easier to solve" than the original one since the starting surface is closer to the expected one.
Since the "first" initialization surface is planar, it is obvious that a "flattened" surface is easier to be reliably reconstructed. It is also clear that a surface flattened with respect to the light direction appears brighter (Figure 2), since surface normals progressively tend to the light direction.
Moreover, it has been demonstrated [24] that by initializing the functional with a surface that roughly represents the

expected one is a better strategy when confronted with the use of planar initialization.
On the light of these observations, generating from the input image a set of images with an increasing level of brightness (in such a set the darker image is the original one) allows 1) to use planar initialization only for the brightest image and 2) to use for the subsequent images an initialization surface closer to the one represented by the analyzed images themselves.
In detail, the devised procedure consists of the following steps:

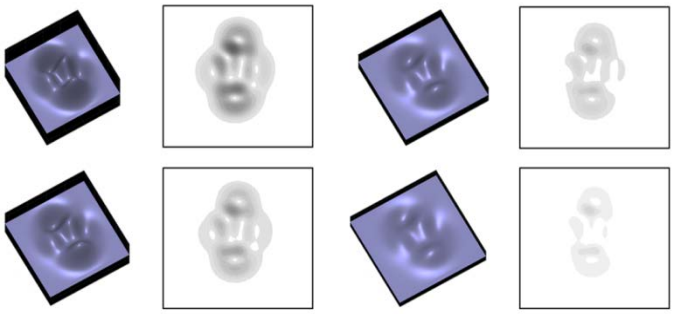

Figure 2- Peaks with flattened surface and the correspondent image with light direction $\vec{L} = [0,0,1]$.

Step 1 - A set of k images is created by increasingly brightening the input image. The images are sorted in ascending order of brightness (so that the first one to be used is the brighter one while the last one corresponds to the original image). Even if conceptually the set of images could be obtained by increasing the brightness with a ΔB step equal to 1, this would involve, in the worst case, 255 sub-problems to be solved. To reduce the computational cost, a good compromise is to use a set of 10 images. Since the lighter image is considered reached when about 94% of pixels have brightness value equal to 255 (i.e. average brightness B_L, excluding the background, equal to 240), and called B_0 the average brightness of the original image, it results:

$$\Delta B = \frac{B_0 - B_L}{10} \tag{11}$$

Step 2 - The first sub-problem, corresponding to the brightest image, is solved by applying Eq. 10 and using the planar initialization (planar surface perpendicular to the light direction).

Step 3 - The obtained solution is used as initialization to solve the following sub-problem.

Step 4 - Step 3 is iterated until the original image is analyzed.

Each step is solved using the BarzilaiBorwein not monotonous algorithm [25] that can be considered effective since the SFS problem is a typical unconstrained problem. Moreover, this method has been proved to be satisfying in terms of speed and accuracy to solve these types of problems. The main issue in applying such an optimization algorithm is to find an optimal criterion for stopping the minimization process.
In this paper two criteria are adopted:
- The first one evaluates the gradient of the functional (Eq. 12);
- The second one evaluates the relative error between two consecutive iterations x_k and x_{k-1} (Eq. 13).

$$\|\nabla F\| < toll_1 \tag{12}$$

$$\frac{\|x_k - x_{k-1}\|}{\|x_k\|} < toll_1 \tag{13}$$

III. Results

In order to assess the effectiveness of the proposed method, three case studies have been carried out. In particular, the results obtained by using the standard planar initialization and the step-by-step procedure are compared both visually and in terms of reconstruction error.
Tests were performed using synthetic images, in which the exact normal map is known. There are two main advantages of using synthetic images: the first is that it is possible to have the same surface with different light sources; the second, extensively used in this work, is that the complete knowledge of the exact normal map is fundamental to compare and validate the obtained solutions. This enables to assess very carefully the error made by each method, to compare the various methods and to obtain an objective evaluation of the goodness of the obtained solution.
The case studies analyzed refer to three surfaces (see Figure 3):

- Donut - size [241 x 241] pixels.
- Pin - size [473 x 420] pixels (see Figure 3).
- Peaks - size [420 x 420] pixels.

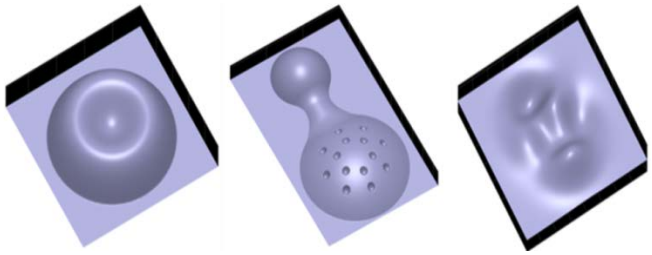

Figure 3 – Ground truth of the surfaces to be retrieved using the proposed method.

Each one of these surfaces is illuminated with two light directions: [0 0 1], front light perpendicular to the plane of the background and [1 1 5], i.e. with a slant angle of 10° and a tilt angle of 45°.
First, the set of images with increasing brightness is built (see for instance Figure 4 where the 10 images created for Pin case study are depicted).

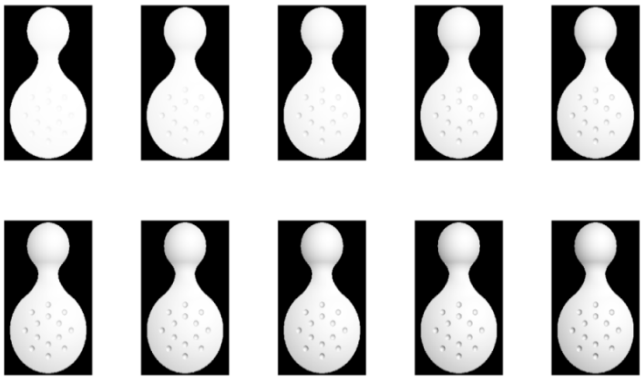

Figure 4 – Pin case study: set of 10 images to be solved (light direction $\vec{L} = [1\ 1\ 5]$).

Then, the 4-steps procedure described in the previous section is accomplished to retrieve the final surface. Tests have been carried out by crossing various parameters, as the weight λ used for the constraint and the tolerance $toll_1$ adopted for the stopping criterion in BarzilaiBorwein algorithm. In this way, it is possible to take into account many configurations of the SFS problem.In Figure 5 some results of reconstruction using the proposed method are depicted together with the results obtained by applying the standard method based on planar initialization. The final reconstruction of the surface is made starting from the solution calculated at the end of the procedures using the strategy described in [26].

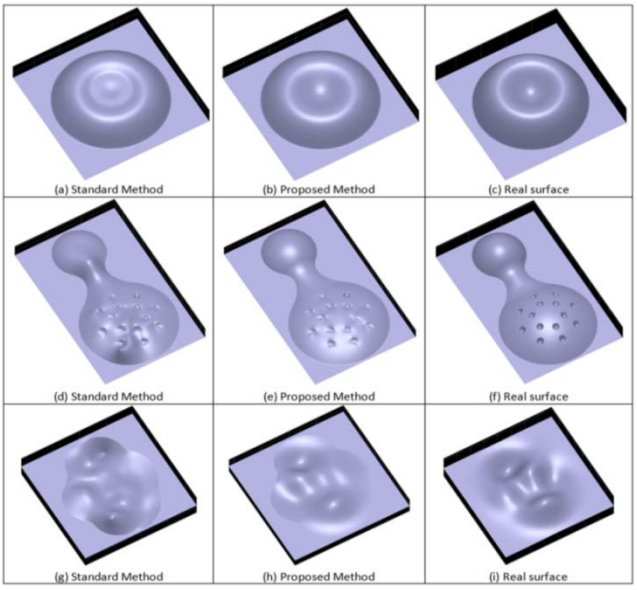

Figure 5 - (a), (b) and (c) are the Donut with light direction $\vec{L} = [0, 0, 1]$, λ=0.1 and $\text{toll}_1 = 10^{-2}$. (d), (e) and (f) are the Pin with $\vec{L} = [1, 1, 5]$, λ=0.01 and $\text{toll}_1 = 10^{-5}$. (g), (h) and (i) are the Peaks with $\vec{L} = [1, 1, 5]$, λ=0.1 and $\text{toll}_1 = 10^{-4}$.

The better performance of the proposed method can be visually deduced; in fact, the reconstructed surface has more details and is more similar to the ground truth.

A numerical comparison between the two methods is achievable by defining two kinds of errors. The first one, namely the "mean absolute deviation error", is defined as the average value of the norm of the difference between the exact normal and the evaluated one:

$$err_1 = \frac{1}{n \cdot m} \sum_{(i,j)\in\Omega} \left\| \vec{N}(i,j) - \vec{\tilde{N}}(i,j) \right\| \tag{14}$$

Where n and m are the number of rows and columns of the image, $\vec{N}(i,j)$ is the true normal map and $\vec{\tilde{N}}(i,j)$ is the achieved one.

The second error is defined as the average of the angle between the exact normal and the evaluated one. Since normal maps are composed by normal vectors, the dot product between the normals coincides with the cosine of the angle ϑ between them:

$$\vartheta(i,j) = \cos^{-1}\left(\vec{N}(i,j) \cdot \vec{\tilde{N}}(i,j)\right) \ \forall\ (i,j) \in \Omega \tag{15}$$

In this way it is possible to define the error as follows:

$$err_2 = \frac{1}{n \cdot m} \sum_{(i,j)\in\Omega} \vartheta(i,j) \tag{16}$$

The results of the two types of error (err_1 anderr_2) are evaluated in the solution calculated at the end of the procedures and before reconstructing the surface.

In Tables from 1 to 6 (see Annex 1) a comparison of measured errors for the proposed method (PM) and the standard one (SM) is described.

Both errors show a substantial improvement of the proposed method over the standard one except for the Donut case with $\vec{L} = [1\ 1\ 5]$, λ=0.1 and $toll_1 = 10^{-4}$, 10^{-5} and 10^{-6}.

To further evaluate the numerical difference between the proposed method and the standard one it is also possible to define the relative errors as follows:

$$re_1 = \frac{err_1(PM) - err_1(TM)}{err_1(PM)} \tag{17}$$

$$re_2 = \frac{err_2(PM) - err_2(TM)}{err_2(PM)} \tag{18}$$

Where $err_1(PM)$ and $err_2(PM)$ are the errors of the proposed method, while $err_1(SM)$and $err_2(SM)$ are the errors of the standard one. In Tables from 7 to 9, the comparison between the proposed method and the standard one in terms of relative error are shown.

Table 1: Comparison of performance (%) – Donut.

		re_1				re_2			
		[0 0 1]		[1 1 5]		[0 0 1]		[1 1 5]	
$toll_1$	λ	0.1	0.01	0.1	0.01	0.1	0.01	0.1	0.01
10^{-2}		-574,80	-160,98	-131,48	-335,74	-576,56	-161,01	-132,46	-355,91
10^{-3}		-148,94	-261,85	-94,08	-454,35	-148,95	-261,89	-95,68	-478,33
10^{-4}		-125,28	-250,60	16,09	-537,69	-125,28	-250,63	16,13	-557,52
10^{-5}		-19,50	-74,50	4,70	-171,69	-19,50	-74,50	4,77	-178,56
10^{-6}		-1,41	-5,76%	1,12	-112,57	-1,41	-5,76	1,14	-117,48

Table 2: Comparison of performance (%) – Pin.

		re_1				re_2			
		[0 0 1]		[1 1 5]		[0 0 1]		[1 1 5]	
$toll_1$	λ	0.1	0.01	0.1	0.01	0.1	0.01	0.1	0.01
10^{-2}		-40,07	-27,80	-22,43	-81,33	-39,95	-27,68	-22,21	-80,05
10^{-3}		-83,25	-45,45	-61,47	-130,30	-83,84	-45,71	-62,33	-134,27
10^{-4}		-11,43	-140,83	-52,35	-176,47	-11,37	-141,79	-52,20	-180,72
10^{-5}		-18,36	-35,85	-11,19	-153,86	-17,57	-35,94	-11,15	-156,53
10^{-6}		-8,88	-27,03	-1,03	-134,95	-8,24	-27,08	-1,03	-137,44

Table 3: Comparison of performance (%) – Peaks.

		re_1				re_2			
		[0 0 1]		[1 1 5]		[0 0 1]		[1 1 5]	
$toll_1$	λ	0.1	0.01	0.1	0.01	0.1	0.01	0.1	0.01
10^{-2}		-79,14	-78,42	-129,96	-1,10	-79,44	-79,02	-124,97	-1,09
10^{-3}		-72,40	-79,09	-567,00	-136,45	-72,83	-79,71	-591,24	-136,08
10^{-4}		-63,15	-73,30	-599,22	-105,78	-63,41	-73,77	-622,06	-106,64
10^{-5}		-61,10	-36,49	-165,93	-58,52	-61,23	-36,65	-171,38	-59,09
10^{-6}		-61,51	-33,48	-124,64	-51,40	-61,69	-33,48	-128,78	-53,28

IV. Conclusions

The present work proposed a novel strategy to improve the reconstruction of a surface starting from a single image. As known, minimization-based SFS procedures may converge towards a solution that does not coincide with the global minimum. In fact, if the iterative algorithm starts from an initial guess that is too far from the actual solution, it may takes a lot of iteration to come up to a solution. Even worse, since the result is obtained using local minimization algorithms, it may do not correspond with the global minimum.

To overcome these issues, the proposed strategy breaks with the standard approach since it splits the retrieving process in multiple steps, each one of them corresponds with an easy sub-problem to solve that provides a proper initialization for the following one. The solution of the last sub-problem coincides with the solution of the original problem. More in detail, each step solves an SFS problem relative to a brightened version of the input image, so that the solution surface is actually a flattened version of the definitive one. Passing from one step to the following one, the image is darkened until the last step, in which the image corresponds to the original one. Since the initialization at the beginning is planar, this strategy is meant to be successful in overcoming the issue related to convergence of the minimization that has been faced in this work.

To validate this procedure, the method was tested on a set of case studies, using several input images relative to 3 different synthetic surfaces with 2 alternative lightings and 12 different settings. Since the original surfaces are known, it has been possible to compare both normal maps and depth maps directly with the real ones. In order to evaluate the performance of this procedure, the same tests have been carried out using the standard approach.

In light of the results, the improvements obtained seem substantial, reducing the relative error committed up to six times. The proposed method is able to produce better results in terms of both numerical error and surface reconstruction. Only in a few cases the standard method and the proposed one behave in the same manner. In future works, this strategy will be further tested on additional case studies, in order to confirm the results shown in this work and handmade drawings will be finally considered. Though shading in this kind of drawings, differently from synthetic images, is inexact, authors believe that shading analysis can still be useful and help recover at least the global shape of the represented object and/or curvature constraints (e.g. tangency) among contiguous regions of the object itself.

ANNEX 1 – TABLES 1-6

Table 4: err_1 - Donut.

	L = [0 0 1]				L = [1 1 5]			
	λ=0.1		λ=0.01		λ=0.1		λ=0.01	
$toll_1$	PM	SM	PM	SM	PM	SM	PM	SM
10^{-2}	5,57639E-03	3,76296E-02	5,41376E-03	1,41286E-02	4,60939E-02	1,06699E-01	6,19278E-02	2,69846E-01
10^{-3}	5,01423E-03	1,24826E-02	3,89871E-03	1,41075E-02	3,61785E-02	7,02159E-02	5,15794E-02	2,85931E-01
10^{-4}	5,47432E-03	1,23326E-02	3,79262E-03	1,32969E-02	4,54100E-02	3,81037E-02	4,00743E-02	2,55550E-01
10^{-5}	9,95373E-03	1,18950E-02	6,78292E-03	1,18361E-02	6,57649E-02	6,26734E-02	5,22039E-02	1,41833E-01
10^{-6}	1,09978E-02	1,11524E-02	1,03791E-02	1,09773E-02	6,81437E-02	6,73772E-02	6,62929E-02	1,40916E-01

Table 5: err_2 - Donut.

	L = [0 0 1]				L = [1 1 5]			
	λ=0.1		λ=0.01		λ=0.1		λ=0.01	
$toll_1$	PM	SM	PM	SM	PM	SM	PM	SM
10^{-2}	5,57728E-03	3,77334E-02	5,41392E-03	1,41308E-02	4,61858E-02	1,07364E-01	6,21315E-02	2,83264E-01
10^{-3}	5,01511E-03	1,24849E-02	3,89887E-03	1,41096E-02	3,62192E-02	7,08751E-02	5,16981E-02	2,98985E-01
10^{-4}	5,47540E-03	1,23348E-02	3,79283E-03	1,32988E-02	4,54714E-02	3,81379E-02	4,01283E-02	2,63851E-01
10^{-5}	9,95530E-03	1,18970E-02	6,78356E-03	1,18376E-02	6,60667E-02	6,29158E-02	5,23265E-02	1,45762E-01
10^{-6}	1,09995E-02	1,11542E-02	1,03802E-02	1,09785E-02	6,84878E-02	6,77051E-02	6,66059E-02	1,44852E-01

Table 6: err_1 - Pin.

	L = [0 0 1]				L = [1 1 5]			
	λ=0.1		λ=0.01		λ=0.1		λ=0.01	
$toll_1$	PM	SM	PM	SM	PM	SM	PM	SM
10^{-2}	6,20026E-02	8,68440E-02	6,26886E-02	8,01144E-02	9,23989E-02	1,13127E-01	1,15015E-01	2,08554E-01
10^{-3}	4,27118E-02	7,82699E-02	5,47653E-02	7,96572E-02	5,97568E-02	9,64877E-02	9,89113E-02	2,27796E-01
10^{-4}	2,92924E-02	3,26394E-02	3,32822E-02	8,01547E-02	3,79512E-02	5,78173E-02	7,81139E-02	2,15959E-01
10^{-5}	2,61440E-02	3,09444E-02	3,19427E-02	4,33937E-02	4,66688E-02	5,18902E-02	4,44522E-02	1,12847E-01
10^{-6}	2,84040E-02	3,09267E-02	3,41609E-02	4,33937E-02	4,87477E-02	4,92495E-02	4,80312E-02	1,12847E-01

Table 7: err_2 - Pin.

	L = [0 0 1]				L = [1 1 5]			
	λ=0.1		λ=0.01		λ=0.1		λ=0.01	
$toll_1$	PM	SM	PM	SM	PM	SM	PM	SM
10^{-2}	6,24013E-02	8,73307E-02	6,32023E-02	8,06979E-02	9,37350E-02	1,14550E-01	1,17238E-01	2,11085E-01
10^{-3}	4,28198E-02	7,87187E-02	5,50613E-02	8,02299E-02	6,01204E-02	9,75951E-02	1,00395E-01	2,35194E-01
10^{-4}	2,94619E-02	3,28113E-02	3,33578E-02	8,06565E-02	3,82030E-02	5,81466E-02	7,88932E-02	2,21469E-01
10^{-5}	2,64737E-02	3,11248E-02	3,20293E-02	4,35405E-02	4,69523E-02	5,21897E-02	4,46933E-02	1,14651E-01
10^{-6}	2,87398E-02	3,11088E-02	3,42619E-02	4,35405E-02	4,90378E-02	4,95409E-02	4,82856E-02	1,14651E-01

Table 8: err_1 - Peaks.

	L = [0 0 1]				L = [1 1 5]			
	λ=0.1		λ=0.01		λ=0.1		λ=0.01	
$toll_1$	PM	SM	PM	SM	PM	SM	PM	SM
10^{-2}	6,01748E-02	1,07798E-01	6,14991E-02	1,09728E-01	8,35773E-02	1,92199E-01	1,93558E-01	1,95679E-01
10^{-3}	5,91592E-02	1,01993E-01	6,03640E-02	1,08106E-01	2,65856E-02	1,77325E-01	1,19747E-01	2,83139E-01
10^{-4}	6,64086E-02	1,08343E-01	6,14047E-02	1,06414E-01	2,95113E-02	2,06347E-01	1,38788E-01	2,85600E-01
10^{-5}	8,67289E-02	1,39717E-01	9,17136E-02	1,25179E-01	7,98369E-02	2,12309E-01	1,73148E-01	2,74480E-01
10^{-6}	8,91664E-02	1,44011E-01	9,94083E-02	1,32687E-01	9,45102E-02	2,12309E-01	1,68774E-01	2,55531E-01

Table 9: err_2 - Peaks.

	L = [0 0 1]				L = [1 1 5]			
	λ=0.1		λ=0.01		λ=0.1		λ=0.01	
$toll_1$	PM	SM	PM	SM	PM	SM	PM	SM
10^{-2}	6,07212E-02	1,08959E-01	6,20591E-02	1,11098E-01	8,61959E-02	1,93914E-01	1,95287E-01	1,97416E-01
10^{-3}	5,96887E-02	1,03162E-01	6,08914E-02	1,09430E-01	2,66012E-02	1,83879E-01	1,24496E-01	2,93912E-01
10^{-4}	6,70027E-02	1,09490E-01	6,19311E-02	1,07619E-01	2,95256E-02	2,13193E-01	1,43330E-01	2,96177E-01
10^{-5}	8,77334E-02	1,41452E-01	9,26335E-02	1,26582E-01	8,01691E-02	2,17564E-01	1,78439E-01	2,83888E-01
10^{-6}	9,02103E-02	1,45861E-01	1,00578E-01	1,34247E-01	9,50987E-02	2,17564E-01	1,72182E-01	2,63924E-01

REFERENCES

[1] Carfagni M., Furferi R., Governi L., Palai M., Volpe Y., "3D reconstruction problem": An automated procedure (2011) Applications of Mathematics and Computer Engineering - American Conference on Applied Mathematics, AMERICAN-MATH'11, 5th WSEAS International Conference on Computer Engineering and Applications, CEA'11, pp. 99-104.

[2] Furferi R., Governi L., Palai M., Volpe Y., "3D model retrieval from mechanical drawings analysis" (2011) International Journal of Mechanics, 5 (2), pp. 91-99.

[3] Volpe Y., Furferi R., Governi L., Tennirelli G., Computer-based methodologies for semi-automatic 3D model generation from paintings (2014) International Journal of Computer Aided Engineering and Technology, 6 (1), pp. 88-112.

[4] Furferi R., Governi L., Palai M., Volpe Y., Multiple Incident Splines (MISs) algorithm for topological reconstruction of 2D unordered point clouds (2011) International Journal of Mathematics and Computers in Simulation, 5 (2), pp. 171-179.

[5] J.-D. Durou, M. Falcone, M. Sagona, Numerical methods for shape-from-shading: A new survey with benchmarks. Comput. Vis. Image Und. 109, 22-43 (2008);

[6] R. Zhang, P.-S. Tsai, J. E. Cryer, M. Shah - Shape From Shading - A Survey, IEEE Transactions on Pattern Analysis and Machine Intelligence archive, Volume 21 Issue 8, August 1999, Page 690-706;

[7] B.K.P. Horn, M.J. Brooks, The variational approach to shape from shading, Computer Vision, Graphics, and Image Processing 33 (2) (1986) 174–208;

[8] Y.G. Leclerc, A.F. Bobick, The direct computation of height from shading, in: Proceedings of the IEEE Conference on Computer Vision and Pattern Recognition, Maui, HI, USA, 1991, pp. 552–558;

[9] P. Daniel, J.-D. Durou, From deterministic to stochastic methods for shape from shading, in: Proceedings of the Fourth Asian Conference on Computer Vision, Taipei, Taiwan, 2000, pp. 187–192;

[10] B.K.P. Horn, Shape from Shading: A Method for Obtaining the Shape of a Smooth, Opaque Object from One View. PhD thesis, Massachusetts Inst. of Technology (1970);

[11] J.A. Sethian, R. Kimmel, Optimal Algorithm for Shape from Shading and Path Planning. J. Math. Imaging Vision 14, 237-244 (2001);

[12] A.P. Pentland, Local Shading Analysis, IEEE Trans. Pattern Analysis and Machine Intelligence, vol. 6, pp. 170-187, 1984;

[13] A. Pentland, Shape Information from Shading: A Theory about Human Perception, Proc. Int'l Conf. Computer Vision, pp. 404-413, 1988;

[14] P.S. Tsai, M. Shah, Shape from Shading Using Linear Approximation, Image and Vision Computing J., vol. 12, no. 8, pp. 487-498, 1994;

[15] P. Daniel, J.D. Durou, From deterministic to stochastic methods for shape from shading. In: Proc. 4th Asian Conf. on Comp. Vis., Taipei, Taiwan, 187-192 (2000).

[16] R.T. Frankot, R. Chellappa, A method for enforcing integrability in shape from shading algorithms. IEEE Trans. Pattern Anal. Mach. Intell. 10, 439-451 (1988).

[17] B.K.P. Horn, M.J Brooks, Shape from Shading. MIT Press (1989).

[18] L. Governi, R. Furferi, L. Puggelli, Y. Volpe, Improving surface reconstruction in Shape from Shading using easy-to-set boundary conditions, International Journal Of Computational Vision And Robotics.

[19] Furferi, R., Governi, L., Volpe, Y., Puggelli, L., Vanni, N., &Carfagni, M. (2014). From 2D to 2.5 D ie from painting to tactile model. *Graphical Models*, 76(6), 706-723.

[20] Frankot, R.T.; Chellappa, R. (1988) - "A Method for Enforcing Integrability in Shape from Shading Algorithms", IEEE Transaction Pattern Analysis and Machine Intelligence, Vol. 10, pp.439-451.

[21] Zheng, Q.; Chellappa, R. (1991) - "Estimation of Illuminant Direction, Albedo, and Shape from Shading", IEEE Transactions on Pattern Analysis and Machine Intelligence, Vol. 13, No. 7, pp. 680-702.

[22] K. Ikeuchi, B. Horn, Numerical Shape from Shading and Occluding Boundaries, Artificial Intelligence Volume 17, Issues 1–3, August 1981, Pages 141–184.

[23] B. Horn, M. Brooks, The Variational Approach to Shape from Shading, Computer Vision, Graphics, and Image Processing.

[24] L. Governi, R. Furferi, L. Puggelli, Y. Volpe, Digital Bas-Relief Design: a Novel, Shape From Shading-Based Method. Computer-Aided Design and Applications 11. 153-164 (2014).

[25] S. Bellavia, L. Governi, A. Papini, L. Puggelli, Quadratic Penalty Methods for Shape from Shading, Conference in Numerical Analysis 2014 (NumAn 2014).

[26] T.-P. Wu, J. Sun, C.-K. Tang, H.-Y. Shum, Interactive Normal Reconstruction from a Single Image, SIGGRAPH Asia '08 ACM SIGGRAPH Asia 2008 papers.

Prof. **Monica Carfagni** (F'61) graduated in 1986 in Mechanical Engineering with Honours from the University of Florence. In 1990 she obtained the PhD. Title in the Research in Applied Mechanics from the University of Bologna. In 1989 she started working for the University of Florence as a researcher in the field of machine design. In 1992 she was given the title of Associate Professor of Industrial Design from the Polytechnic of Milan and in 1993 she was transferred to the University of Florence, where she currently chairs Technical Computer Graphics. In 2002 she was given the title of Full Professor of Industrial Design from the Engineering Faculty of the University of Florence where she had the role of Dean of the Mechanical and Industrial Technology Department from 2007 to 2012. Main research activities are on Computer Aided Design, Image Processing, Industrial Diagnostics, Virtual Prototyping, FE simulation and Computer Aided Tolerancing. In the last 5 years she worked on Computer-based methods and tools based on 2D and 3D machine vision for industrial, textile and agronomical process and product control and inspection and in Computer-based methods for modelling and simulation of industrial processes.

Dr. Puggelli(M'85)concluded his PhD activity in industrial engineering in December 2014. He currently work at the University of Florence, Department of Industrial Engineering, as post doctorate researcher in mechanical engineer. His main interests involve the 3D modelling and Reverse Engineering techniques. In particular, his latest research activity is focused on the *Shape from Shading* techniques, especially dealing with non-synthetic images.